Design and Fabrication of PTFE Substrate-Integrated Waveguide Butler Matrix for Short Millimeter Waves

Mitsuyoshi KISHIHARA[†a)], *Member*, **Kaito FUJITANI**[††], **Akinobu YAMAGUCHI**[††],
Yuichi UTSUMI[††], *Nonmembers*, **and Isao OHTA**[†††], *Member*

SUMMARY We attempt to design and fabricate of a 4×4 Butler matrix for short-millimeter-wave frequencies by using the microfabrication process for a polytetrafluoroethylene (PTFE) substrate-integrated waveguide (SIW) by the synchrotron radiation (SR) direct etching of PTFE and the addition of a metal film by sputter deposition. First, the dimensions of the PTFE SIW using rectangular through-holes for G-band (140-220 GHz) operation are determined, and a cruciform 90 ° hybrid coupler and an intersection circuit are connected by the PTFE SIW to design the Butler matrix. Then, a trial fabrication is performed. Finally, the validity of the design result and the fabrication process is verified by measuring the radiation pattern.

key words: *microstructure, X-ray lithography, dielectric loaded waveguides, Butler matrix, millimeter wave circuits*

1. Introduction

Microparts such as mechatronics, optics, and fluidics have been developed using various microfabrication technologies such as laser cutting and lithography. In microwave engineering, trial fabrications of hollow waveguide horn antennas by a process with SU-8 photoresist [1] and hollow waveguides of laser-cured resin with copper electroplating [2] have been reported. In recent years, many attempts have been made to realize various circuit elements by using additive manufacturing technology (AMT) [3].

It has been reported that polytetrafluoroethylene (PTFE) microstructures can be fabricated by direct exposure to X-ray from synchrotron radiation (SR) [4]–[6]. The fabrication process for a PTFE-based waveguide for millimeter waves by the SR direct etching of PTFE and the addition of a Au film by sputter deposition and electroplating has also been proposed [7]. The fabrication process is considered useful for constructing waveguide-integrated circuits for millimeter-wave and submillimeter-wave bands. However, at higher frequencies of more than 100 GHz, the PTFE-filled waveguide circuit becomes weaker than paper

[†]The author is with the Faculty of Computer Science and System Engineering, Okayama Prefectural University, Soja-shi, 719–1197 Japan.
[††]The authors are with the Laboratory of Advanced Science and Technology for Industry, University of Hyogo, Hyogoken, 678–1205 Japan.
[†††]The author is with the University of Hyogo, Kobe-shi, 651–2197 Japan.
a) E-mail: kisihara@c.oka-pu.ac.jp

and bends or snaps off easily unless it is fixed with resin [8].

A waveguide whose sidewalls are replaced with densely arranged metallic posts has been proposed. This type of waveguide is called a post-wall waveguide (PWW) [9]–[11] or a substrate-integrated waveguide (SIW) [12]–[14]. In this study, the design of a 4×4 Butler matrix for short millimeter waves is attempted using a PTFE-based SIW structure. The SIW structure is favorable in terms of the shape retention of the microstructure and the high degree of freedom in the design [15]. First, the dimensions of the PTFE SIW using rectangular through-holes are determined for G-band (140-220 GHz) operation. Then, the cruciform 90 ° hybrid coupler (3 dB coupler) and an intersection circuit (0 dB coupler) of the PTFE SIW structure analogous to the circuits in Ref. [8] are connected to design a Butler matrix. Then, a trial fabrication of the PTFE SIW Butler matrix is performed by the above-mentioned fabrication process utilizing the SR direct etching of PTFE and Au coating by sputter deposition and electroplating. Finally, the radiation pattern of the Butler matrix is measured to validate the design result and the fabrication process.

2. Design of Butler Matrix

2.1 Propagation Constant of PTFE SIW

The basic structure of the PTFE SIW is shown in the inset in Fig. 1. The rectangular areas ($R_x \times R_y$) in the PTFE sheet with relative permittivity ε_r represent through-holes that act as the side walls of the waveguide. They are arranged with spacing s and width W. The surface of the through-holes and the upper and bottom planes of the PTFE sheet must be metal. The thickness of the PTFE sheet is much less than the wavelength used in its circuit system, the propagation and nonpropagation modes excited in the PTFE SIW are TE_{n0}-like modes. Namely, the PTFE SIW has the same propagation characteristics as a conventional rectangular waveguide. In this study, the use of PTFE sheets with a thickness of 0.40 mm is assumed.

The calculated frequency dependences of the phase and attenuation constants of the PTFE SIW for the G-band is shown in Fig. 1. They are derived from the S-parameters of two straight SIW sections with different lengths which correspond to "Thru" and "Line" connections, based on the TRL calibration technique [16]. In this study, the S-parameters of the straight SIW section are analyzed using
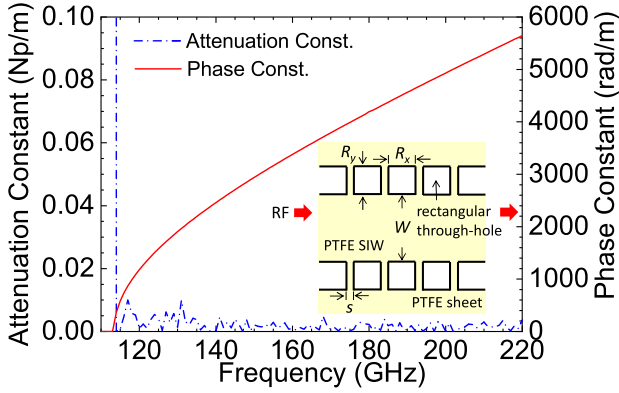
Fig. 1 Calculated phase and attenuation constants of PTFE SIW for G-band (W = 0.90 mm, s = 0.20 mm, R_x = R_y = 0.30 mm, ε_r = 2.04). Inset is basic structure of PTFE SIW. (view of H-plane)
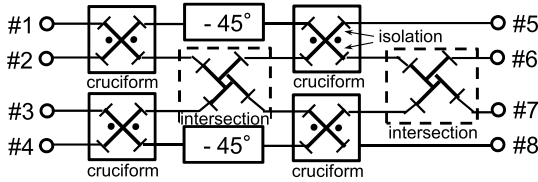

Fig. 2 Block diagram of 4×4 Butler matrix.

Fig. 3 Structure of PTFE SIW cruciform coupler. (view of H-plane)

Fig. 4 Structure of PTFE SIW intersection coupler. (view of H-plane)

H-plane planar circuit approach [17], where the impedance boundary is used for the outer boundaries to include the leakage loss. The dimensions W, s, R_x, and R_y are adjusted so as to have the same cutoff frequency as that of the G-band standard waveguide. The spacing s and the dimensions of the through-hole, R_x and R_y, should be selected so that the leakage field remains sufficiently small. As a result, W = 0.90 mm, s = 0.20 mm, and R_x = R_y = 0.30 mm are obtained under the assumption that the relative permittivity of the PTFE sheet, ε_r, is 2.04. In the analysis, the PTFE sheet is treated as lossless and the metal parts are treated as perfect conductors. In Fig. 1, the TE$_{10}$-like mode occurs at f_c = 113 GHz. No higher-order mode occurs within the G-band frequency range. It is found that the attenuation constant is less than 0.01 Np/m at the operation band, and the present configuration can greatly suppress the radiation loss due to the structure.

2.2 Circuit Components of Butler Matrix

Figure 2 shows a block diagram of a 4×4 Butler matrix. It is constructed from four 90 ° hybrid couplers, two 45° phase shifters, and two crossings. In this study, a simplified cruciform coupler is utilized as the 90 ° hybrid coupler. As the crossing structure, an H-plane waveguide intersection circuit is adopted. Namely, the PTFE SIW 4×4 Butler matrix can be constructed from four cruciform couplers, two intersection circuits, and phase-shifting waveguides. The output phase differences among ports #5 to #8 vary depending on which port (#1 to #4) is used as the input port.

Figure 3 shows the structure of a PTFE SIW cruciform coupler. It consists of four input/output PTFE SIWs con-
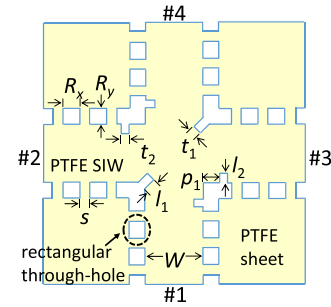
nected at right angles. The configuration of the PTFE SIW is depicted with the rectangular through-holes. Two rectangular slits of length l_1 are arranged symmetrically on the diagonal line of the crossed region to control the directivity. The rectangular slit of length l_2 at each port is inserted as a matching element. The dimensions W, s, R_x, and R_y are the parameters associated with the PTFE SIW, while the dimensions l_1, l_2, t_1, t_2, and p_1 are the parameters for the cruciform coupler. The dimensions for the G-band PTFE SIW cruciform 3 dB coupler are obtained from Ref. [8] as l_1 = 0.21 mm, l_2 = 0.16 mm, t_1 = t_2 = 0.20 mm, and p_1 = 0.28 mm. Assuming that port #1 is an input port, ports #2 and #3 become an isolation port and a coupling port, respectively. The phase difference between the outputs #3 and #4 becomes 90 °. The fractional bandwidth of 14.6% is achieved for the return loss better than 20 dB and the power-split imbalance less than 0.5 dB.

Figure 4 displays the structure of the PTFE SIW intersection circuit. The structure exhibits rotational symmetry, where the length of one side is given by a. The 0 dB coupling characteristics can be obtained by optimizing the dimensions and positions of the matching elements represented by t, p_2, and l. Unfortunately, since the intersection circuit does not exhibit reflection symmetry, it is difficult to connect to each circuit and align the ports at equal intervals. In this work, circular bends of angle θ are added to the intersection circuit and the port positions are centered. The radii of the bends are represented by R_θ. Two bends are connected at each port, and then a straight section of length l_θ is
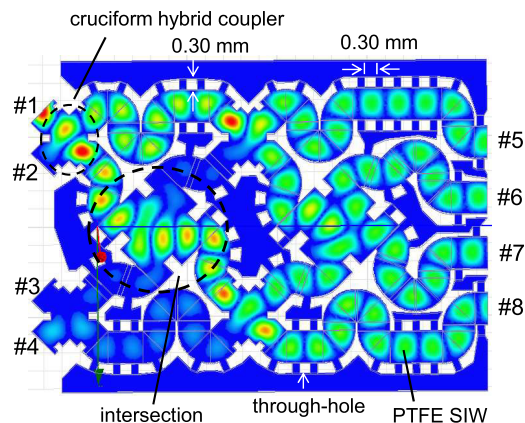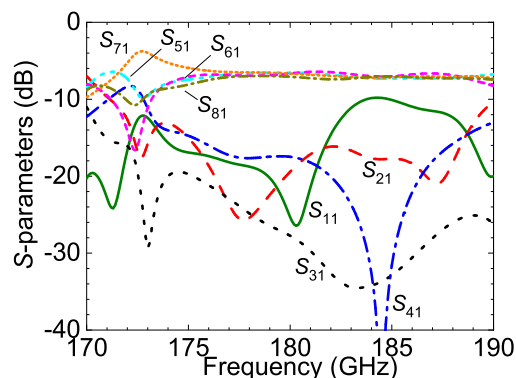
Fig. 5 Configuration of PTFE SIW 4×4 Butler matrix and electric field distribution excited at port #1.

(a)

(b)

Fig. 6 Frequency characteristics of S-parameters of PTFE SIW 4×4 Butler matrix. (a) Magnitudes. (b) Output phase differences (input port: #1).

inserted between them to center the ports. The dimensions for the G-band PTFE SIW intersection circuit are given as $a = 2.40$ mm, $p_2 = 0.57$ mm, $t = 0.32$ mm, $l = 0.39$ mm, $\theta = 65°$, $R_\theta = 0.55$ mm, and $l_\theta = 0.127$ mm. The fractional bandwidth is 5.5% for the return loss better than 20 dB and the insertion loss less than 0.5 dB.

2.3 Layout of Circuit Components

Figure 5 shows the layout of a 4×4 Butler matrix consisting of four cruciform couplers, two intersection circuits, and PTFE SIWs for the connection and phase shift. It also shows the electric field distribution when the input is from port #1. This layout is obtained by calculating the frequency characteristics of the S-parameters using the EM simulator HFSS and connecting each component while checking the phase shift. Through-holes are basically squares with a side of 0.30 mm, however, the spacing and dimensions are adjusted to avoid interference with curved sections and adjacent circuits.

Figure 6 shows the frequency characteristics of the S-parameters of the PTFE SIW 4×4 Butler matrix. In the calculation, conductor loss (Au: $4.1×10^7$ S/m) and dielectric loss (PTFE: $\tan\delta = 0.0002$) are considered. It is found that the reflection S_{11} and the isolation characteristics S_{21}-S_{41} indicate below −15 dB for the frequency range 175.3 GHz to 181.9 GHz, and the outputs S_{51}-S_{81} become −7.9 dB to −6.1 dB as shown in Fig. 6 (a). Since the reflection S_{11} of the present Butler matrix is degraded above 182 GHz, there is no margin compared to the waveguide type in Ref. [8] which has the upper frequency limit of 188 GHz. The output imbalance 1.8 dB is also a little large compared to 0.35 dB in Ref. [8]. When inputted from port #1, the phase differences between the adjacent ports become almost 45 ° at 180 GHz, as shown in Fig. 6 (b). The phase differences contain the maximum deviation of 10.4 ° at 180 GHz (0.4 ° in Ref. [8]). Although these deviation may affect the performance of the Butler matrix and the operation is limited to narrowband, the present circuit works as a Butler matrix at 180 GHz.
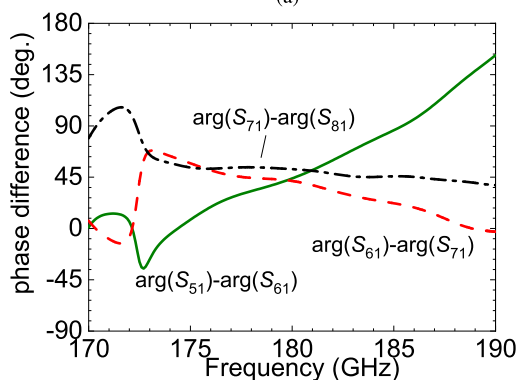
In this paper, output ports #5 to #8 of the 4×4 Butler matrix are integrated with the PTFE-filled waveguide horn antennas. The validity of the designed Butler matrix is evaluated by measuring its radiation pattern. The dimensions of the horn antenna are 1.54 mm length to the aperture, 1.05 mm aperture width, and 1.10 mm arrangement interval. Since the total horn width is 4.35 mm, the far-field distance of the designed 4×4 Butler matrix is estimated as 22.9 mm. For ports #1 to #4, a pattern is provided so that an input waveguide can be connected to any one of them at the time of trial fabrication.

3. Fabrication

The fabrication process for the PTFE SIW Butler matrix consists of the SR direct etching of the PTFE sheet, the RF sputtering of Au, and electroplating that are the same process as Ref. [8]. In this study, the pattern where the input/output port is #1 is fabricated. Figure 7 (a) shows a photograph of the PTFE structure covered with the Au film obtained after sputtering and electroplating. The amount of X-ray exposure is 2560 Asec (time required: 2.5 h). The apertures of the horn antennas are not covered with a Au film, as shown in Fig. 7 (b). They are realized by covering the side surface with a PTFE piece during sputtering. Among ports #2 to #4, the ports to which no input is connected are short-circuited. This short-circuited condition is
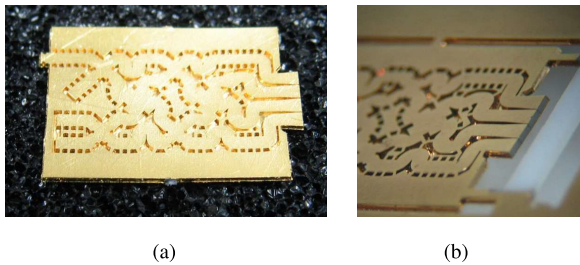
Fig. 7 Fabricated Butler matrix. (a) Butler matrix with surrounding PTFE frame removed (input port #1). (b) Area of apertures of horn antennas.

Fig. 8 Measured H-plane radiation patterns of PTFE SIW 4×4 Butler matrix at 180 GHz. Measuring port: #1.

adopted, knowing that the reflection will occur at the end. Since the matching terminations could not be prepared, the measurement is compared with the simulation result including the reflected waves.

4. Measurement

The same measurement system as Ref. [8] is prepared using a frequency tripler (VDI WR5.1×3 Broadband Tripler) and a detector (VDI WR5.1 Zero-Bias Detector). A vector network analyzer (Agilent E8361C) is used as the V-band source. When the V-band signal (60 GHz) is input to the tripler, the G-band signal (180 GHz) can be obtained. A conical horn is utilized for the transmission antenna, and the Butler matrix is connected to the detector. The Butler matrix is put on the rotator such that antenna radiation patterns can be measured. The distance between the antennas is 10 cm and their height is 5 cm. The received signal is observed as DC voltage.

The H-plane radiation pattern is measured at 180 GHz for the fabricated Butler matrix. The result is shown in Fig. 8. 0 ° is set as the direction of the transmitting antenna. The measured values are normalized using the maximum value. The solid line is the measured radiation pattern, and it is found that the direction of the main beam roughly agrees with the HFSS simulation result (chain line). Because the arrangement interval of the horn antennas is not optimized in this design, the direction of the main beam (−10 °) is meaningless. However, it is confirmed that the phases from the each circuit component are synthesized correctly, and the fabricated structure functions as a Butler matrix.

From the view point of fabrication accuracy, the stencil mask used in this work contains a dimensional error of ±7.5 μm (15 μm at maximum). It would cause an error in the propagation length. Since the guide wavelength of the SIW is 1.53 mm at 180 GHz, the dimensional error 15 μm corresponds to a phase shifting of 3.5 °. Because the amounts of the phase shifting are adjusted by the lengths of the SIWs and each component is connected by them to form the Butler matrix, it is considered that these phase errors may appear in the final phase differences. The phase error may also occur for each SIW component, and then the each phase error would be summed. A detailed evaluation of the phase errors included in the circuit will be a task in future work.
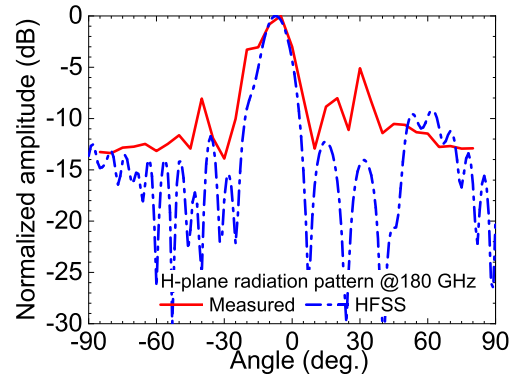
5. Conclusion

The trial fabrication of a PTFE SIW 4×4 Butler matrix for short millimeter waves was attempted by SR direct etching, the sputter deposition of a metal, and electroplating. The Butler matrix was constructed from four cruciform 3 dB couplers, two intersection circuits, and phase-shifting SIWs. The radiation pattern of the fabricated 4×4 Butler matrix was measured. It was confirmed that the direction of the main beam agrees with the HFSS simulation result. The present fabrication process and the PTFE SIW are considered useful for integrating the circuit components at millimeter-wave and submillimeter-wave frequencies.

References

[1] J.W. Digby, C.E. McIntosh, G.M. Parkhurst, B.M. Towlson, S. Hadjiloucas, J.W. Bowen, J.M. Chamberlain, R.D. Pollard, R.E. Miles, D.P. Steenson, L.S. Karatzas, N.J. Cronin, and S.R. Davies, "Fabrication and characterization of micromachined rectangular waveguide components for use at millimeter-wave and terahertz frequencies," IEEE Trans. Microw. Theory Tech., vol.48, no.8, pp.1293–1302, Aug. 2000.

[2] J. Hirokawa, M. Zhang, T. Tomura, and M. Ando, "94GHz-band fabrication of a hollow waveguide of laser-curing resin with copper-electroplating on the internal walls," Proc. of IEICE Society Conf., p.166, B-1-166, Sept. 2008 (in Japanese).

[3] V. Laur, M.K. Abboud, A. Maalouf, D. Palessonga, A. Chevalier, and J. Ville, "Heat-resistant 3D printed microwave devices," Proc. 2018 Asia-Pacific Microwave Conf. pp.1318–1320, Nov. 2018.

[4] Y. Zhang, T. Katoh, M. Washio, H. Yamada, and S. Hamada, "High aspect ratio micromachining Teflon by direct exposure to synchrotron radiation," Appl. Phys. Lett., vol.67, no.6, pp.872–874, Aug. 1995.

[5] Y. Ukita, K. Kanda, S. Matsui, and Y. Utsumi, "Fabrication of PTFE microstructure using synchrotron radiation direct etching for microfluidics application," Proc. 50th International Conference on Electron, Ion, and Photon Beam Technology & Nanofabrication, pp.509–510, 2006.

[6] A. Yamaguchi, H. Kido, Y. Ukita, M. Kishihara, and Y. Utsumi, "Anisotropic pyrochemical microetching of poly(tetrafluoroethylene) initiated by synchrotron radiation-induced scission of molecule bonds," Appl. Phys. Lett., vol.108, no.5, 051610, Feb. 2016.

[7] M. Kishihara, Y. Ukita, Y. Utsumi, and I. Ohta, "Fabrication of a PTFE-filled waveguide for millimeter-wave components using SR direct etching," Microsyst. Technol., vol.14, pp.1417–1422, Feb. 2008.

[8] M. Kishihara, M. Takeuchi, A. Yamaguci, Y. Utsumi, and I. Ohta, "Fabrication of integrated PTFE-filled waveguide Butler matrix for short millimeter-wave by SR direct etching," IEICE Trans. Electron., vol.E101-C, no.6, pp.416–422, June 2018.

[9] J. Hirokawa and M. Ando, "Single-layer feed waveguide consisting of posts for plane TEM wave excitation in parallel plates," IEEE Trans. Antennas Propagat., vol.46, no.5, pp.625–630, May 1998.

[10] M. Ando, J. Hirokawa, T. Yamamoto, A. Akiyama, Y. Kimura, and N. Goto, "Novel single-layer waveguides for high-efficiency millimeter-wave arrays," IEEE Trans. Microw. Theory Tech., vol.46, no.6, pp.792–799, June 1998.

[11] Y. She, T.H. Tran, K. Hashimoto, J. Hirokawa, M. Ando, "Loss of post-wall waveguides and efficiency estimation of parallel-plate slot arrays fed by the post-wall waveguide in the millimeter-wave band," IEICE Trans. Electron., vol.E94-C, no.3, pp.312–320, March 2011.

[12] D. Deslandes and K. Wu, "Integrated microstrip and rectangular waveguide in planar form," IEEE Microw. Wireless Compon. Lett., vol.11, no.2, pp.68–70, Feb. 2001.

[13] D. Deslandes and K. Wu, "Substrate integrated waveguide leaky-wave antenna: concept and design considerations," Proc. Asia Pacific Microwave Conf., vol.1, pp.346–349, Dec. 2005.

[14] E. Moldovan, R.G. Bosisio, and K. Wu, "W-band multiport substrate-integrated waveguide circuits," IEEE Trans. Microw. Theory Tech., vol.54, no.2, pp.625–632, Feb. 2006.

[15] M. Kishihara, M. Takeuchi, A. Yamaguci, Y. Utsumi, and I. Ohta, "Design and fabrication of PTFE substrate integrated waveguide coupler by SR direct etching," IEICE Trans. Electron., vol.E104-C, no.9, pp.446–454, Sept. 2021.

[16] D.M. Pozar, Microwave Engineering, Second Edition, John Wiley & Sons, 1998.

[17] M. Kishihara, I. Ohta, K. Okubo, and J. Yamakita, "Analysis of post-wall waveguide based on H-plane planar circuit approach," IEICE Trans. Electron., vol.E92-C, no.1, pp.63–71, Jan. 2009.